Preparation and Characterization of Tapioca Starch-Poly(lactic acid)-Cloisite NA$^+$ Nanocomposite Foams

Siew-Yoong Lee, Milford A. Hanna

Industrial Agricultural Products Center, Biological Systems Engineering Department, University of Nebraska-Lincoln, Nebraska 68583-0730

Received 16 August 2007; accepted 20 November 2007
DOI 10.1002/app.27730
Published online 18 August 2008 in Wiley InterScience (www.interscience.wiley.com).

ABSTRACT: Tapioca starch, poly(lactic acid), and Cloisite NA$^+$ nanocomposite foams, with four clay contents (1, 3, 5, 7, wt %), were prepared by melt-intercalation method. Selected structural, thermal, physical, and mechanical properties were characterized using X-ray diffraction (XRD), scanning electron microscopy, differential scanning calorimetry, and an Instron universal testing machine, respectively. XRD results indicated that the 1 wt % nanocomposite foam did not show the characteristic basal reflection of the nanoclay. The 3, 5, and 7 wt % nanocomposite foams produced a mixture of intercalated and tactoid structures. The d_{001}-spacing of 3, 5, 7 wt % nanocomposite foams produced increases of 11.40, 11.15, and 10.67 Å, respectively, compared to that of the pristine clay. The morphological study showed that the nanocomposite foams exhibited a noticeably reduced cell size, more compact cells, and increased cell density. Increasing clay content caused a decrease in melting temperature (T_m). Bulk spring index and bulk compressibility were influenced ($P < 0.05$) significantly with the addition of different amounts of clay. © 2008 Wiley Periodicals, Inc. J Appl Polym Sci 110: 2337–2344, 2008

Key words: compatibility; foam extrusion; organoclay; nanocomposites; differential scanning calorimetry

INTRODUCTION

Poly(lactic acid) (polylactate or polylactide) (PLA) is a polyester, and is synthesized from L- and D-lactic acid, which are produced from the fermentation of sugar and (poly)saccharides such as sugar feedstocks and corn, wheat, and other starch sources. The lactic acid is converted to PLA either by ring-opening polymerization or by condensation polymerization. PLA is insoluble in water and has good moisture and grease resistances. Its mechanical properties can be modified by varying its molecular weight and crystallinity.[1] PLA is used widely as a biodegradable and renewable plastic for uses in service ware, grocery, waste-composting bags, mulch films, controlled release matrices for fertilizers, pesticides, and herbicides.[2] However, PLA is expensive because of the complicated synthesis.

Starch is a natural polymer, inexpensive, readily available, and often used as a filler for the replacement of petroleum-derived synthetic polymers to decrease environmental pollution. However, starch has severe limitations because of its solubility and poor water-resistance, making starch products very sensitive to the relative humidity at which they are stored and used.[3] Starch-polyester blends are being produced with the objective of maintaining the excellent physical properties of the polyesters while reducing cost. A process was developed at the University of Nebraska-Lincoln to produce starch-based plastic foam with 70% starch combined with a variety of ingredients and plastics.[4] Fang and Hanna[5] found that addition of PLA to regular and waxy corn starches improved the physical and mechanical properties of the foams. Recently, formation of nanocomposites with the aim of improving functional properties has become popular. One of the most promising nanocomposites is formed from organic polymer and inorganic clay minerals consisting of layered silicates.

Polymer nanocomposites are a class of reinforced polymers containing small quantities (1–5 wt %) of nanometric-sized clay particles. Smectite-type clays, such as hectorite, synthetic mica, and montmorillonite, are employed as fillers to enhance the properties of composites. The functional properties of the nanocomposites are improved markedly compared to those of the unfilled polymer or conventional composites. These improvements included high moduli,[6,7] increased tensile strength[8] and thermal stability,[9] decreased gas permeability,[10] flammability[11] and water absorbance,[12] and increased biodegradability.[13]

Of the four methods (solution intercalation, *in situ* polymerization, melt intercalation, and template synthesis) which have been used to synthesize nanocomposites, melt intercalation is the most appealing

Correspondence to: M. A. Hanna (mhanna1@unl.edu).
Contract grant sponsor: University of Nebraska Agricultural Research Division and Hatch Act, USDA.

approach because of its versatility, compatibility with polymer processing equipment, and because it is an environmentally friendly process that requires no solvent and is suitable for industrial uses.[14,15] In melt intercalation the clay and polymer are added together above the melting temperature of the polymer. They may be held at this temperature for a period of time, put under shear, or other conditions to encourage intercalation and exfoliation of the clay.[16]

Generally, polymer/layered silicate composites are divided into three main types: tactoid, intercalated, and exfoliated nanocomposites. In a tactoid, the polymer is unable to intercalate between the silicate sheets and the properties of the composites stay in the same range as the traditional microcomposites. Intercalated nanocomposites occur when a small amount of polymer moves into the gallery spacing between the silicate platelets. When the silicate layers are dispersed completely and uniformly in a continuous polymer matrix, an exfoliated or delaminated structure is formed.[17] The intercalated and exfoliated nanocomposites currently are of primary interest because their properties are significantly improved, even at low clay concentrations. However, the formation of intercalated or exfoliated nanocomposites depends on the type of organoclay,[9,18] the clay content,[19,20] and the processing conditions.[21]

The objective of this study was to prepare tapioca starch (TS)/PLA/Cloisite NA^+ nanocomposite foams of different clay contents via melt-intercalation and to investigate the influence of clay content on selected structural, morphological, thermal, physical, and mechanical properties of the foams.

EXPERIMENTAL

Materials

Semicrystalline PLA resin of MW_n 85,000 was produced by Cargill (Minneapolis, MN). It contained ~ 93% L-lactide, 2% D-lactide, and 5% mesolactide. It was in the form of 2–4 mm spheres. The thermal properties measured by differential scanning calorimetry (DSC) showed a melting point of 174°C. The true density of PLA resin was 1.22 g/cm^3. PLA usually is used as amorphous material in molded products because of its low rate of crystallization, though it is semicrystalline polymer. Commercially available TS was purchased from Starch Tech (Minnesota, MN). TS was agglomerated into spherical granules of 2–4 mm diameter to facilitate feeding into the extruder. The moisture content of the TS was adjusted to 18%, dry basis, with distilled water prior to extrusion. TS and 10% PLA were blended with 0.5% sodium bicarbonate, 0.5% citric acid, and clay in a Hobart mixer (Model C-100, Horbart Corp., Troy, OH) and stored in plastic jars prior to extrusion.

TABLE I
Clay Contents Used in the Preparation of Tapioca Starch-PLA (TS/PLA) Nanocomposite Foams

Samples	Cloisite NA^+ (wt%)
TS	–
TS/PLA	–
TS/PLA+NA1	1
TS/PLA+NA3	3
TS/PLA+NA5	5
TS/PLA+NA7	7

PLA content of 10% was selected based on preliminary experiments. Fang and Hanna[5] used three levels of polymer content (10, 25, 40%) in their study of mechanical properties of starch-based foams. They found that at 10% PLA content, the foams possessed the highest spring index and intermediate compressibility and Young's modulus values. They concluded that for practical applications, the bulk mechanical properties were more meaningful. Sodium bicarbonate and citric acid were added to degrade the biodegradable polymer into chains of between 1000 and 100,000 Da or ~ 500 to 50,000 monosaccharide groups to promote expansion.[4]

Table I shows the six different formulations used. Natural montmorillonite under the trade name of Cloisite NA^+ (cation exchange capacity (CEC) = 92.6 m equiv./100 g) was obtained from Southern Clay Products (Gonzalez, TX). The particle size range of the nanoclay was 2–13 nm. PLA and the nanoclay were dried in the oven at 70°C for at least 24 h.

Extrusion

A twin-screw extruder (Model DR-2027-K13, C. W. Brabender, S. Hackensack, NJ) with corotating mixing screws (Model CTSE-V, C. W. Brabender) was used to conduct extrusions. The conical screws had diameters decreasing from 43 to 28 mm along their length of 365 mm from the feed end to the exit end. On each screw, there was a mixing section, in which small portions of the screw flights were cut away. The mixing section enhanced the mixing action and also increased the residence time of the sample in the barrel. A 150-rev/min screw speed was used for all extrusions. The temperature at the feeding section was maintained at 50°C, the second barrel section at 120°C, the third barrel section at 150°C, and die section at 170°C. A 3-mm diameter die nozzle was used to produce continuous cylindrical rope-like extrudates which were cut by a rotary cutter. The extruder was controlled by a Plasti-Corder (Type FE 2000, C. W. Brabender). Data including screw rotating speeds, barrel temperature profiles, pressure profiles, and torque readings were recorded for subsequent

analyses. Extrusion conditions selected were based on preliminary studies and previous experiments.

X-ray diffraction

The X-ray patterns of the samples were obtained using a Rigaku D/Max- B X-ray diffractometer (Tokyo, Japan) with Cu Kα radiation (λ = 1.544 Å) at a voltage of 40 kV and 30 mA. Samples were scanned in the range of diffraction angle 2θ = 2°–10° with a scan speed of 1°/min at room temperature.

Scanning electron microscopy

The morphologies of TS/PLA and TS/PLA nanocomposite foams were observed under a scanning electron microscopy (SEM) (Hitachi S-3000N, Tokyo, Japan). Before testing, the samples were mounted on SEM stubs with double-sided adhesive tape and then coated with platinum under vacuum to make the sample conductive.

Differential scanning calorimetry

DSC measurements were performed with a Mettler DSC (Columbus, OH). About 10 mg of dried, ground samples were placed in aluminum sample pans. The samples were heated from 25 to 200°C at a heating rate of 10°C/min in a nitrogen atmosphere. The sample was kept at 200°C for 1 min for the elimination of the previous heat history and was subsequently cooled to 25°C at 10°C/min. The melting temperature (T_m) was determined as the temperature at the maximum value of the melting peak.

Unit density

Unit densities of the foams were determined using a glass bead displacement method originally developed for determining the volume of cookies[22] with modifications.[23] Glass beads of 0.1 mm diameter were used as the displacement medium. A mean value was obtained by averaging five replicates.

Bulk spring index

Bulk spring index (BSI) measurements were made using an Instron universal testing machine (Model 5566, Instron Engineering Corp., Canton, MA). A cylindrical aluminum container with a volume of 365 cm^3 (6.93 cm in diameter and 9.68 cm in depth) was used to confine the bulk samples.[24] The forces required to initially compress the samples to 80% of their original volumes and the forces required to recompress the same samples 1 min after releasing the initial load were recorded. BSI was calculated by dividing the recompression force by the initial compression force and has an ideal value of 1. A mean value was obtained by averaging five replicates.

Bulk compressibility

Bulk compressibility was calculated using the same data collected in the BSI test. It was calculated by dividing the peak force required to compress (deform) the sample by 80% [to 20% of their original dimension (diameter)] by the initial axial cross-sectional area of the foams.[24] A mean value was obtained by averaging five replicates.

Statistical analyses

All results reported are means of two or more replications. The radial expansion ratio, unit density, BSI, and bulk compressibility data were analyzed using the general linear models (GLM) in SAS analysis program (SAS Institute, Cary, NC). Duncan's multiple range tests were conducted to check for significant ($P < 0.05$) differences between treatment groups.

RESULTS AND DISCUSSION

A preliminary study using Cloisite Na$^+$ at 3 wt % was conducted to determine the extent of intercalation and its influence on the structural, morphological, thermal, physical, and mechanical properties of the nanocomposite foams. In this study, four different relative contents of Cloisite Na$^+$ at 1, 3, 5, and 7 wt % were added to the TS/PLA matrices to study the most suitable clay content and its implication on these properties.

Structural properties of TS/PLA/Cloisite NA$^+$ nanocomposites

Wide-angle X-ray diffraction (WAXD) is a classical method for determining the gallery height (*d*-spacing distance) in clay particles.[25] The *d*-spacing can be determined from the diffraction peak in the XRD patterns, and be expressed by Bragg's equation ($\lambda = 2d_{001}\sin\theta$) where d_{001} is the interplanar distance of the (001) diffraction face, θ is the diffraction position, and λ is the wavelength.[14] During melt intercalation, the insertion of polymer into the organoclay galleries forces the platelets apart and increases the *d*-spacing, resulting in a shift of the diffraction peak to lower angles.

WAXD diffractograms for the four nanocomposite foams are shown in Figure 1. Line a in Figure 1 is the diffraction spectra of pristine Cloisite NA$^+$ clay. The pristine Cloisite NA$^+$ clay had one peak at the diffraction angle 2θ of 7.22°. The WAXD diffractogram for the 1 wt % clay content nanocomposite did

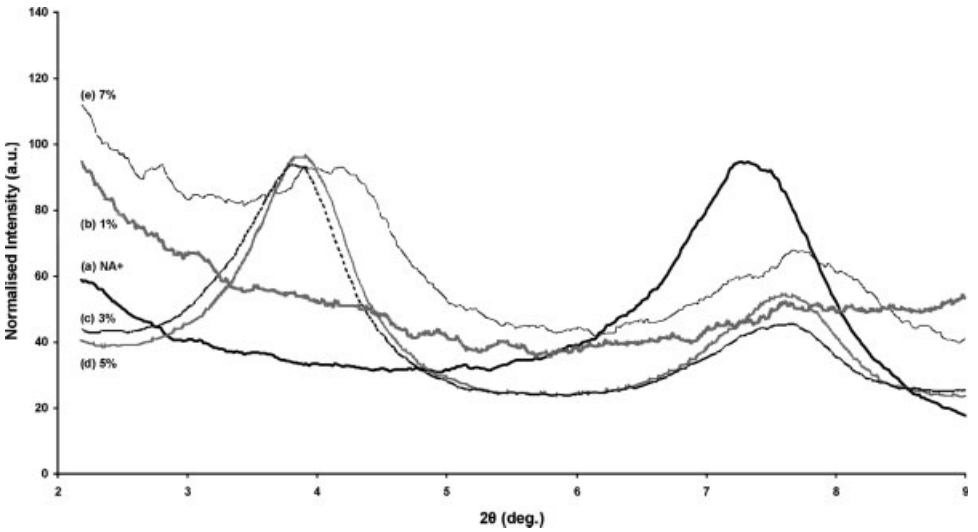

Figure 1 X-ray patterns of (a) Cloisite NA^+, and its nanocomposite foams with tapioca starch and PLA (TS/PLA) at different clay contents (b) 1 wt %, (c) 3 wt %, (d) 5 wt %, and (e) 7 wt %.

not show the characteristic basal reflection of the nanoclay as shown by line b in Figure 1. This is possibly evidence of exfoliation because of the nonexistence of the peak. Since the concentration of the nanoclay used was low, at 1 wt %, and at this time no other characterizations were available to be employed to confirm the exfoliated structure for proper interpretation of the data.

Lines c–e in Figure 1 are the spectra of the 3, 5, 7 wt % clay content nanocomposites having two peaks, at (001) and (002) *d*-spacings. In these three nanocomposites, the first diffraction peaks (001) *d*-spacings were observed to shift to lower angles compared to that of pristine nanoclay, indicating that intercalation of TS/PLA polymer into the nanoclay layers occurred. The first diffraction peaks (001) *d*-spacings for 3, 5, 7 wt % clay occurred at $2\theta = 3.74^\circ$, 3.78°, and 3.86°, respectively. Intercalation was greater with the filler contents of 3 and 5 wt % clay content, as shown by the sharp ascent of the diffraction profile baselines at low angles indicating that they had similar intercalation properties. The first diffraction peaks (001) *d*-spacings for both of these intercalated nanocomposites were narrow, indicating a strong intercalated behavior and a high stacking order of the successive clay layers in the nanocomposites. Similar occurrences were observed by Kumar et al.[26] and Ranade et al.[27]

The higher clay content of 7 wt % tended to have the same diffraction profile, with a slightly higher first diffraction peak (001) *d*-spacing angle at $2\theta = 3.86^\circ$. However, the broader peak indicated some level of reduction in the clay platelets per stack in the polymer matrix. This could have been due to either the processing used or to the favorable interaction between the Cloisite NA^+ clay and the TS/PLA.[26]

The second diffraction peaks (002) *d*-spacings for 3, 5, 7 wt % clay content occurred at $2\theta = 7.52^\circ$, 7.59°, and 7.67°, respectively. These peaks appeared smaller and broader indicating that a small fraction of the clay was still present as agglomerated sheets which contributed to a tactoid structure. The moderate surface polarity of Cloisite Na^+ was responsible for the formation of a partially intercalated TS/PLA nanocomposite. The Na^+ cation gave Cloisite Na^+ the proper hydrophilicity and compatibility with TS which favored partial intercalation. This was due to the polymers being too hydrophobic to migrate into the hydrated Na^+ interlayer space.[28] From the above results, it was concluded that a mixture of intercalated and tactoid structures formed during extrusion of TS, PLA, and Cloisite Na^+. Similar observations were reported by Di et al.[25]

The peak of the pristine Cloisite NA^+ clay ($2\theta = 7.22^\circ$) shifted to 3.74° for the 3 wt % nanocomposite foam (Table II). The d_{001}-spacing of 3 wt % nanocomposite foam was 23.62 Å, a 11.40 Å increase compared to that of the original Cloisite NA^+ (12.22 Å). The d_{001}-spacings ofthe 5 and 7 wt % nanocomposite

TABLE II
Diffraction Peaks, d_{001}-Spacings and Δd_{001}-Spacings of Cloisite NA^+ and its Nanocomposite Foams with Tapioca Starch (TS/PLA) at Different Clay Contents

Materials	Diffraction peak (2θ, degree)	d_{001}-Spacings (Å)	Δd_{001}-Spacings (Å)
NA	7.22	12.22	–
TS/PLA+NA1	No Peak	–	–
TS/PLA+NA3	3.74	23.62	11.40
TS/PLA+NA5	3.78	23.37	11.15
TS/PLA+NA7	3.86	22.89	10.67

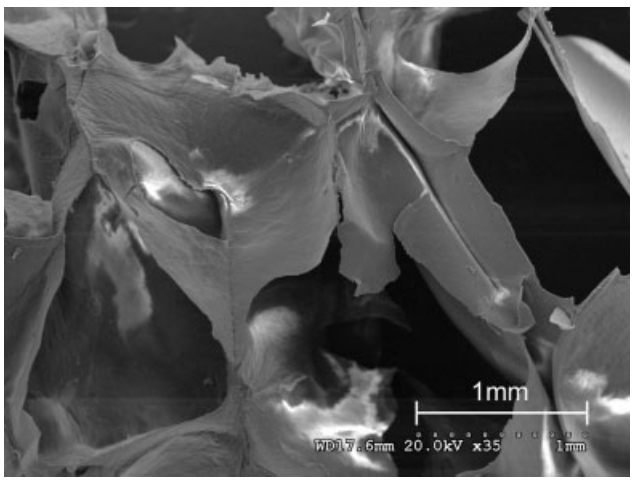

Figure 2 Scanning electron micrograph of tapioca starch and PLA (TS/PLA) composite foam (magnification 35×).

foams were 23.37 and 22.89 Å, respectively. The increase of d_{001}-spacings of 5 and 7 wt % clay content nanocomposite foams were 11.15 and 10.67 Å, respectively. These data show that the nanoclay was intercalated to lesser extents as the clay content increased.

It is believed that the greater the d_{001}-spacings, the greater the interaction of polymer molecular chain with clay layered silicate.[14] The interactions between a polymer and nanoclay depend on the compatibility of the surface polarities of the polymer and the organoclay.[29] Polar-type intercalations are also critical for the formation of intercalated or exfoliated nanocomposites via polymer melt intercalation.[30]

Typical SEM micrographs of TS/PLA foam (Fig. 2), and 1, 3, 5, and 7 wt % clay nanocomposites (Fig. 3) are presented. The TS/PLA foam exhibited cell structure with large cells. The nanocomposites showed a noticeably reduced cell size, more compact cells, and increased cell density. This indicated that the dispersed organoclay particles acted as nucleating sites for cell formation.[31] The higher clay content nanocomposite foams had more compact cells and higher cell densities than the lower clay content nanocomposite foams.

Thermal property of TS/PLA/Cloisite NA$^+$ nanocomposites

Melting temperature (T_m) of TS/PLA and its nanocomposite foams were investigated by DSC. TS foam had a T_m of 162.4°C. The raw PLA was transparent beads and had a T_m of 173.9°C. The TS/PLA foam had a T_m of 165.7°C as shown in Table III. Even though the foam consisted of 90% TS, the T_m of the TS/PLA foam was close to that of the pure PLA, indicating that the thermal effect resulted from PLA, not the starch.[32] Figure 4 shows the DSC thermographs of the nanocomposites which show endothermic melting peaks above 160°C. Similar curves were obtained for all the nanocomposites. At 1 wt % clay

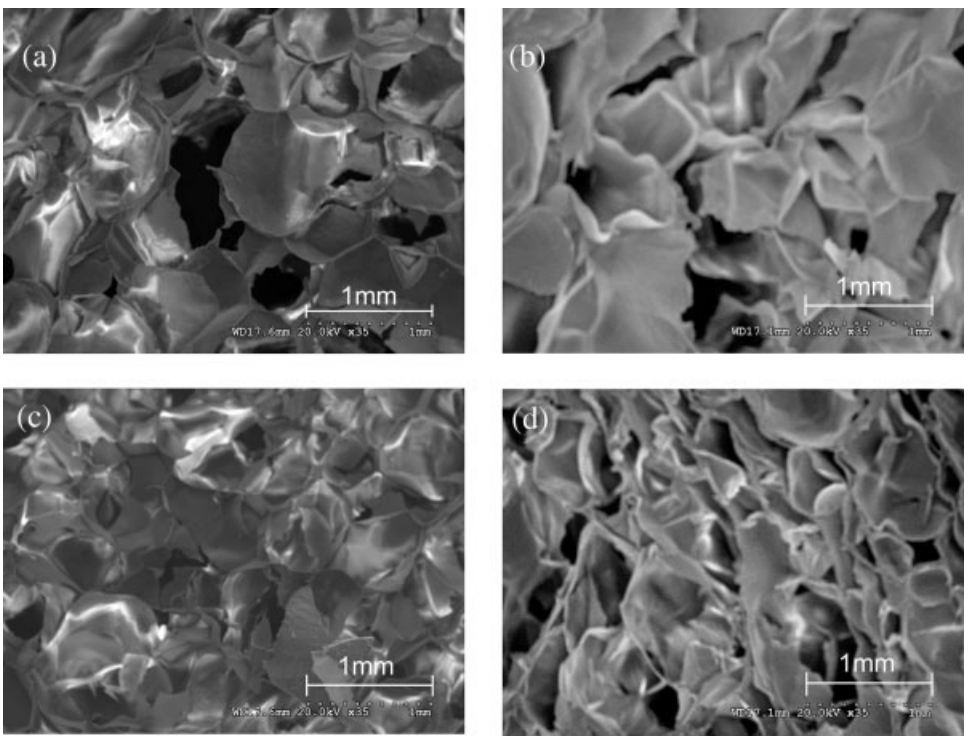

Figure 3 SEM micrographs of TS/PLA/Cloisite NA$^+$ nanoclay foam with (a) 1 wt % clay, (b) 3 wt % clay, (c) 5 wt % clay, and (d) 7 wt % clay (magnification 35×).

TABLE III
Thermal, Physical, and Mechanical Properties of Tapioca Starch (TS), Tapioca Starch-PLA (TS/PLA), and its Nanocomposite Foams with Different Cloisite NA$^+$ Contents

	Thermal property	Physical and mechanical property		
Materials	T_m (°C)	Unit density (kg/m^3)	Bulk spring index	Bulk compressibility (MPa)
TS	162.4	75.0 ± 0.016^a	0.931 ± 0.026^b	14.3 ± 4.212^a
TS/PLA	165.7	48.0 ± 0.009^b	0.947 ± 0.013^{ab}	7.25 ± 0.540^c
TS/PLA+NA1	171.8	55.8 ± 0.005^b	0.961 ± 0.002^a	7.32 ± 0.256^c
TS/PLA+NA3	176.0	56.2 ± 0.004^b	0.953 ± 0.002^a	5.87 ± 0.262^c
TS/PLA+NA5	172.8	58.4 ± 0.006^b	0.947 ± 0.011^{ab}	7.39 ± 0.293^c
TS/PLA+NA7	160.7	82.2 ± 0.006^a	0.956 ± 0.001^a	11.9 ± 0.550^b

$^{a–c}$ means with same letter within a column indicate no significant ($P > 0.05$) difference by Duncan multiple range test.

concentration, the T_m was 171.8°C as shown in line a of Figure 4. The T_m of 3, 5, and 7 wt % nanocomposite foams were 176.0, 172.8, and 160.7°C, as shown by lines b, c, and d in Figure 4, respectively. These temperatures were relatively high considering that the clay concentration was low, indicating that the clay had an influence on the thermal transition of the foam. The decrease in T_m, with increasing clay concentration, could be attributed to the compatibility of this nanoclay with the starch and PLA matrix, which suppressed the crystallization, therefore lowering the T_m.[25] Additionally, the silicate acted as a nucleating agent, causing the viscosity of the matrix to drop, decreasing the T_m.[33] Artzi et al.[19] observed the same occurrence of decreased T_m with increasing clay content. The influence of nanoclay on the reduction of crystallization and melting behavior of PLA became distinct when the concentration of clay was around 3 wt % due to the intercalated nanostructure.[28,34,35] The enthalpy of the melting peak was evaluated for all the nanocomposites. The melting enthalpies for 1, 3, 5, 7 wt % nanocomposite foams were 72.27, 73.63, 78.82, and 81.86 J/g, respectively, indicating that the melting enthalpies increased as the clay concentration increased.

Physical and mechanical properties of TS/PLA/Cloisite NA$^+$ nanocomposites

Physical and mechanical properties of the foams are related strongly to the structure of intermolecular matrices. Unit density is an important physical property of foams. Low unit density is desirable attribute for foams because of the reduced material cost. Pure TS foam had a unit density of 75.0 kg/m^3 (Table III). Addition of PLA had a significant effect on the unit density of TS/PLA foam at 48.0 kg/m^3. This large decrease in unit density could have been the effect of the PLA. The adhesion forces between starch and PLA may have been caused by polar interactions between the two phases, and because hydrogen bonding forces existed between the carbonyl group on PLA and the hydroxyl groups on starch.[36] It was observed that the addition of 1, 3, and 5 wt % clay contents had significant effects on the unit density of the nanocomposite foams as compared to the pure TS foam. However, the highest clay content of 7 wt % produced the highest unit density among all the nanocomposite foams. The 1, 3, and 5 wt % nanocomposite foams had unit densities which were not significantly different from each other at 55.8, 56.2, and 58.4 kg/m^3, respectively. The 7 wt % nanocomposite foam had a unit density of 82.2 kg/m^3, which was not significantly different from the TS foam and significantly different from the 1, 3, and 5 wt % nanocomposite foams. These results indicated that the addition of PLA and clay had an effect on unit density of TS foam.

BSI and bulk compressibility are interrelated properties. BSI relates to resiliency, and refers to the ability of a material to recover its original shape after it has been deformed. A larger BSI indicates a greater degree of rebound of a material after being compressed. Bulk compressibility describes the cushioning ability of a material, and is related to its relative softness or hardness. High BSI and low compressibility are desirable for loose-fill packaging material.[37] Pure TS foam had the lowest BSI of 0.931. Addition of PLA did not have a significant effect on the BSI of TS/PLA foam (0.947). BSI was influenced ($P < 0.05$) significantly by the addition of clay into the TS/PLA

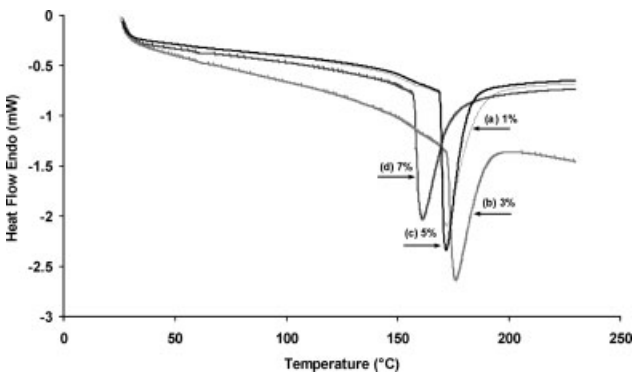

Figure 4 DSC thermographs of tapioca starch-PLA/Cloisite NA$^+$ nanocomposite foams at clay contents of (a) 1 wt %, (b) 3 wt %, (c) 5 wt %, and (d) 7 wt %.

matrix. The 1 wt % nanocomposite foam had the highest BSI of 0.961. The 3, 5, and 7 wt % nanocomposite foams had BSI which were not significantly different from each other at 0.953, 0.947, and 0.956, respectively. The 5 wt % clay content produced a BSI of 0.947 which was similar to the BSI of TS/PLA foam.

Pure TS foam had a significantly higher bulk compressibility of 14.3 MPa. The bulk compressibility decreased to 7.25 MPa, with the addition of PLA. This could have been due to the PLA reacting readily with the starch matrix to form strong interactions between them.[38] Addition of different amounts of clay to the nanocomposites reduced the bulk compressibility significantly ($P < 0.05$). The 1, 3, and 5 wt % clay contents produced bulk compressibilities which were not significantly different from each other at 7.32, 5.87, and 7.39 MPa, respectively. The highest loading of clay (7 wt %) produced a bulk compressibility of 11.9 MPa which was significantly different from the bulk compressibility of the other nanocomposites.

CONCLUSIONS

From the WAXD study, the 1 wt % nanocomposite foam did not show the characteristic basal reflection of the nanoclay. This was possibly evidence of exfoliation because of the nonexistence of the peak. Since the concentration of the nanoclay used was low (1 wt %) and at this time no other characterizations were available to be employed to confirm the exfoliated structure for proper interpretation of the data. The 3, 5, and 7 wt % nanocomposite foams produced a mixture of intercalated and tactoid structures. The d_{001}-spacing of 3 wt % clay content produced an increase of 11.40 Å compared to that of the pristine clay. The d_{001}-spacings of 5 and 7 wt % clay content produced increases of 11.15 and 10.67 Å, respectively. These data show that the nanoclay was intercalated to a lesser extent as clay contents increased. The TS/PLA foam exhibited cell structure with large cells. The nanocomposite foams showed a noticeably reduced cell size, more compact cells, and increased cell density. The higher clay content nanocomposite foams had more compact cells and a higher cell density than the lower clay content nanocomposite foams.

At 1 wt % clay concentration, the T_m was 171.8°C. The T_m of 3, 5, and 7 wt % nanocomposite foams were 176.0, 172.8, and 160.7°C, respectively. The decrease in T_m with increasing clay concentration could be attributed to the compatibility of this nanoclay with the starch and PLA mixture which suppressed the crystallization. It was observed that the addition of 1, 3, and 5 wt % clay contents had significant effects on the unit density of the nanocomposite foams as compared to the pure TS foam.

BSI was influenced ($P < 0.05$) significantly with the addition of different clay contents into the TS/PLA matrix. Addition of different amounts of clay to the nanocomposites reduced the bulk compressibility significantly ($P < 0.05$). The 1, 3, and 5 wt % clay contents produced bulk compressibilities which were not significantly different from each other at 7.32, 5.87, and 7.39 MPa, respectively. The highest loading of clay (7 wt %) produced a bulk compressibility of 11.9 MPa which was significantly different from the bulk compressibility of the other nanocomposites.

Mention of trade names, propriety products, or company name is for presentation clarity only and does not imply endorsement by the authors or the University of Nebraska. The authors wish to thank Dr. Han Chen of the Microscopy Core Facility for the use of SEM and Mr. Brian Jones of the Physics Department for the use of X-ray diffractometer.

References

1. Stevens, E. S. Green Plastics—An Introduction to the New Science of Biodegradable Plastics; Princeton University Press: Princeton, NJ, 2002.
2. Fang, Q.; Hanna, M. A. Ind Crops Prod 1999, 10, 47.
3. Simmons, S.; Thomas E. L. J Appl Polym Sci 1995, 58, 2259.
4. Chinnaswamy, R.; Hanna, M. A. U.S. Pat. 496,895 (1993).
5. Fang, Q.; Hanna, M. A. Trans ASAE 2000, 43, 1715.
6. Lim, Y. T.; Park, O. O. Macromol Rapid Commun 2000, 21, 231.
7. Nam, P. H.; Maiti, P.; Okamoto, M.; Kotaka, T.; Hasegawa, N.; Usuki, A. Polymer 2001, 42, 9633.
8. Dennis, H. R.; Hunter, D. L.; Chang, D.; Kim, S.; White, J. L.; Cho, J. W.; Paul, D. R. Polymer 2001, 42, 9513.
9. Chang, J.-H.; Jang, T.-G.; Ihn, K. J.; Lee, W.-K.; Sur, G. S. J Appl Polym Sci 2003, 90, 3208.
10. Yuen, J.-H.; Bang, G.-S.; Park, B. J.; Ham, S. K.; Chang, J.-H. J Appl Polym Sci 2006, 101, 159.
11. Morgan, A. B. Polym Adv Technol 2006, 17, 206.
12. Chiou, B.-S.; Yee, E.; Wood, D.; Shey, J.; Glenn, G.; Orts, W. Cereal Chem 2006, 83, 300.
13. Ray, S. S.; Yamada, K.; Okamoto, M.; Ueda, K. Polymer 2003, 44, 867.
14. Choi, W. M.; Kim, T. W.; Park, O. O.; Chang, Y. K.; Lee, J. W. J Appl Polym Sci 2003, 90, 525.
15. Li, X. C.; Ha, C.–S. J Appl Polym Sci 2003, 87, 1901.
16. Dean, K.; Yu, L. In Biodegradable Polymers for Industrial Applications; Smith, R., Ed.; CRC Press: Boca Raton, FL, 2005, p 289.
17. Pollet, E.; Paul, M.-A.; Dubois, Ph. In Biodegradable Polymers and Plastics; Kluwer Academic/Plenum Publishers: New York, 2002, p 327.
18. Ammala, A.; Hill, A. J.; Lawrence, K. A.; Tran, T. J Appl Polym Sci 2007, 104, 1377.
19. Artzi, N.; Nir, Y.; Narkis, M.; Siegmann, A. J Appl Polym Sci Part B: Polym Phys 2002, 40, 1741.
20. Nobel, M. L.; Picken, S. J. J Appl Polym Sci 2007, 104, 2146.
21. Tanoue, S.; Hasook, A.; Itoh, T.; Yanou, M.; Iemoto, Y.; Unryu, T. J Appl Polym Sci 2006, 101, 1165.
22. Hwang, M. P.; Hayakawa, K. J Food Sci 1980, 45, 1400.
23. Bhatnagar, S.; Hanna, M. A. ASAE Paper No. 916541, 1991.
24. Fang, Q.; Hanna, M. A. Cereal Chem 2000, 77, 779.
25. Di, Y.; Iannace, S.; Maio, E. D.; Nicolais, L. J Appl Polym Sci Part B: Polym Phys 2005, 43, 689.
26. Kumar, S.; Jog, J. P.; Natarajan, U. J Appl Polym Sci 2003, 89, 1186.

27. Ranade, A.; D'souza, N.; Gnade, B.; Thellen, C.; Orroth, C.; Froio, D.; Lucciarini, J; Ratto, J. A. In Mat Res Soc Symp Proc Vol 791—Mechanical Properties of Nanostructured Materials and Nanocomposites, Ovid'ko, I.; Pande, C. S.; Krishnamoorti, R.; Lavernia, E.; Skandan, G., Eds. Materials Research Society: Warrendale, Pennsylvania, 2004.
28. Paul, M.-A.; Alexandra, M.; Degee, Ph.; Henrist, C.; Rulmont, A.; Dubois, Ph. Polymer 2003, 44, 443.
29. Park, H.-M.; Lee, W.-K.; Park, C.-Y.; Cho, W.-J.; Ha, C.-S. J Mater Sci 2003, 38, 909.
30. Vaia, R. A.; Giannelis, E. P. Macromolecules 1997, 30, 8000.
31. Fujimoto, Y.; Ray, S. S.; Okamoto, M.; Ogami, A.; Yamada, K.; Ueda, K. Macromol Rapid Commun 2003, 24, 457.
32. Sun, X. S. In Bio-based Polymers and Composites; Wool, R. P.; Sun, X. S., Eds.; Elsevier Academic Press: Burlington, MA, 2005.
33. Wang, K. H.; Choi, M. H.; Koo, C. M.; Xu, M.; Chung, I. J.; Jang, M. C.; Choi, S. W.; Song, H. H. J Appl Polym Sci 2002, 40, 1454.
34. Hu, X.; Lesser, A. J. J Appl Polym Sci Part B: Polym Phys 2003, 41, 2275.
35. Pulta, M. Polymer 2004, 45, 8239.
36. Ke, T.; Sun, X. Cereal Chem 2000, 77, 761.
37. Bhatnagar, S.; Hanna, M. A. Trans ASAE 1995, 38, 567.
38. Pluta, M.; Galeski, A.; Alexandre, M.; Paul, M.-A.; Dubios, Ph. J Appl Polym Sci 2002, 86, 1497.